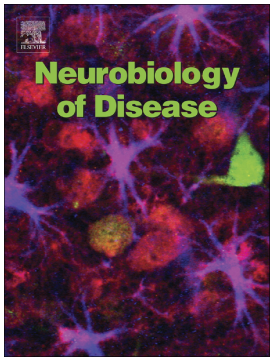

Amplifying mitochondrial function rescues adult neurogenesis in a mouse model of Alzheimer's disease

Kevin Richetin, Manon Moulis, Aurélie Millet, Macarena S. Arràzola, Trinovita Andraini, Jennifer Hua, Noélie Davezac, Laurent Roybon, Pascale Belenguer, Marie-Christine Miquel, Claire Rampon

PII: S0969-9961(17)30051-7
DOI: doi: 10.1016/j.nbd.2017.03.002
Reference: YNBDI 3916

To appear in: *Neurobiology of Disease*

Received date: 6 September 2016
Revised date: 3 March 2017
Accepted date: 8 March 2017

Please cite this article as: Kevin Richetin, Manon Moulis, Aurélie Millet, Macarena S. Arràzola, Trinovita Andraini, Jennifer Hua, Noélie Davezac, Laurent Roybon, Pascale Belenguer, Marie-Christine Miquel, Claire Rampon , Amplifying mitochondrial function rescues adult neurogenesis in a mouse model of Alzheimer's disease. The address for the corresponding author was captured as affiliation for all authors. Please check if appropriate. Ynbdi(2017), doi: 10.1016/j.nbd.2017.03.002

Amplifying mitochondrial function

rescues adult neurogenesis in a mouse model of Alzheimer's disease

Authors: Kevin Richetin[1], Manon Moulis[1], Aurélie Millet[1], Macarena S. Arràzola[1], Trinovita Andraini[1,2], Jennifer Hua[1], Noélie Davezac[1], Laurent Roybon[3], Pascale Belenguer[1], Marie-Christine Miquel[1#] and Claire Rampon[1#]*

Authors affiliations :

[1] Centre de Recherches sur la Cognition Animale, Centre de Biologie Intégrative, Université de Toulouse, CNRS, UPS, France

[2] Department of Physiology, Faculty of Medicine, Universitas Indonesia, Jakarta, Indonesia

[3] Stem Cell Laboratory for CNS Diseases Modeling, Department of Experimental Medical Science, Wallenberg Neuroscience Center, Lund Stem Cell Center and MultiPark, Lund University, BMC A10, 221 84 Lund, Sweden

[#] share senior authorship

*** Corresponding author :** Claire Rampon, UMR5169 CNRS, Centre de Recherches sur la Cognition Animale, Centre de Biologie Intégrative, Université Paul Sabatier, 118, route de Narbonne 31062 Toulouse Cedex 9, France; phone: +33 (0)5 61 55 75 75, e-mail: claire.rampon@univ-tlse3.fr

Running title: Mitochondria support adult neurogenesis

Abstract

Adult hippocampal neurogenesis is strongly impaired in Alzheimer's disease (AD). In several mouse models of AD, it was shown that adult-born neurons exhibit reduced survival and altered synaptic integration due to a severe lack of dendritic spines. In the present work, using the APPxPS1 mouse model of AD, we reveal that this reduced number of spines is concomitant of a marked deficit in their neuronal mitochondrial content. Remarkably, we show that targeting the overexpression of the pro-neural transcription factor *Neurod1* into APPxPS1 adult-born neurons restores not only their dendritic spine density, but also their mitochondrial content and the proportion of spines associated with mitochondria. Using primary neurons, a *bona fide* model of neuronal maturation, we identified that increases of mitochondrial respiration accompany the stimulating effect of *Neurod1* overexpression on dendritic growth and spine formation. Reciprocally, pharmacologically impairing mitochondria prevented *Neurod1*-dependent trophic effects. Thus, since overexpression of *Neurod1* into new neurons of APPxPS1 mice rescues spatial memory, our present data suggest that manipulating the mitochondrial system of adult-born hippocampal neurons provides neuronal plasticity to the AD brain. These findings open new avenues for far-reaching therapeutic implications towards neurodegenerative diseases associated with cognitive impairment.

Keywords: Adult neurogenesis, *Neurod1*, mitochondria, dentate gyrus, Alzheimer's disease.

Introduction

In mammals, new neurons are produced in the hippocampus throughout adult life (Altman and Das, 1965; Eriksson et al., 1998). These neurons become structurally and functionally integrated into the hippocampal circuitry where they contribute to hippocampal-dependent memory processes (Aimone et al., 2011; Gu et al., 2012). Recent data indicate that regulation of mitochondrial function and morphology through fusion and fission events, i.e. mitochondrial dynamics, is part of the cellular program that controls the development and sustains the maturation of new neurons during adulthood (Steib et al., 2014), suggesting that, reciprocally, mitochondrial defects could be associated with altered adult neurogenesis.

Due to neurons distinctive arborescent morphology and high compartmentalization (dendrites, axon, synapses), their functions and survival present a challenge for mitochondria, which must be highly adaptive and move within and between the subcellular compartments involved in neuroplasticity. By generating energy and contributing to calcium and redox homoeostasis, mitochondria are imperative in the fundamental processes that control neuroplasticity, such as neural differentiation (Hagberg et al., 2014), neurite outgrowth and synaptic maturation (Bertholet et al., 2013), neurotransmitter release (Vos et al., 2010), and dendritic remodeling (Cheng et al., 2010; Li et al., 2004; Mattson, 2008). Moreover, as circulating signaling platforms, mitochondria integrate various signals, including deleterious ones, and can ultimately precipitate neurons into apoptosis (Magnifico et al., 2013).

Among neurodegenerative pathologies, Alzheimer Disease (AD) is one of the most common causes of dementia and cognitive impairment in the elderly. Mitochondrial alterations have been reported in the brains of AD patients (Hirai et al., 2001), as well as in transgenic mouse models of AD (Pedrós et al., 2014; Trushina et al., 2012; Xu et al., 2017). More recently, the expression of genes essential for mitochondrial biogenesis, like NRF1 and PGC-1alpha was found to be strongly down-regulated in the hippocampus of the transgenic APPxPS1 mouse model, as early as 3 and 6 months of age (Pedrós et al., 2014). Notably, several studies, including ours, have reported alterations of adult hippocampal neurogenesis in these AD mice (Demars et al., 2010; Hamilton and Holscher, 2012; Taniuchi et al., 2007; Verret et al., 2007). We recently established that morphological development and synaptic integration of adult-born hippocampal neurons of the double transgenic APPxPS1 mouse model of AD could be enhanced by the targeted overexpression of the basic helix–loop–helix transcription factor (bHLH) *Neurod1*, favoring its pro-neural differentiating effects (Richetin et al., 2015). Remarkably, the presence of such highly connected adult-born neurons was sufficient to rescue to normal spatial

memory in APPxPS1 mice (Richetin et al., 2015), emphasizing the need for further investigations of the underlying cellular mechanisms.

Of note, another neurogenic bHLH transcription factor from the NeuroD family, Neurod6, was found to confer tolerance to oxidative stress to differentiated stably transfected PC12 cells, by sustaining neuronal mitochondrial biomass (Uittenbogaard et al., 2010) and ATP levels during the very early stages of neuronal differentiation (Baxter et al., 2009). Similarly, PGC-1alpha-dependent enhancement of mitochondrial biogenesis was demonstrated to play an *sine qua non* role during the formation and maintenance of neuronal dendritic spines (Cheng et al., 2012). Therefore, we hypothesized that the beneficial effect of *Neurod1* overexpression on adult-born neurons could be mediated, at least in part, by an action on mitochondrial biogenesis and/or function. We thus tested this hypothesis in maturating neurons *in vitro* as well as in the APPxPS1 mouse model of AD. In this study, we conclusively identify mitochondria dysfunction as an important contributor of adult neurogenesis alteration in the context of AD pathology, and we demonstrate that this effect can be reversed by *Neurod1* gene delivery through an increase of mitochondrial biogenesis as well as of mitochondria-endowed spines.

Material and Methods

Primary culture of cortical neurons and transfection. All animal procedures were approved by the CNRS/Fédération de Recherche de Biologie de Toulouse Animal Experimentation Ethics Committee (C2EA-01) under the protocol number 01024-01.7. As previously described (Bertholet et al., 2013), cortical neurons were prepared from Day 17 embryos from pregnant Wistar rats (Janvier) dissected after intraperitoneal Pentobarbital (Sigma) anesthesia. Briefly, cortices were microdissected, enzymatically dissociated with papain (10 U/ml, Sigma), dissociated by trituration and filtered through a membrane (70 µm, BD Falcon). Cells were then purified through a BSA solution (8%, Sigma) diluted in Neurobasal A-25 (Invitrogen). Cells (5×10^6) were electroporated after dissociation using the Rat Neuron Nucleofector Kit (Amaxa, Lonza) and three micrograms of pCMMP-IRES2eGFP (to express GFP alone) or pCMMP-*Neurod1*-IRES2eGFP (to co-express GFP and *Neurod1*) plasmids. According to our previous work, transfection efficiency around 36-37% (Bertholet et al., 2013). Cells were plated on 35mm dishes or 12mm glass coverslips in 24 well plates previously coated with poly-D-lysine (0.1 mg/mL, Sigma). Cells were grown in Neurobasal A-25 supplemented with B27 (Invitrogen), 1 mM glutamine, 1% penicillin and streptomycin (1000U/mL, Gibco), 250 U/ml amphotericin (Invitrogen) and 1 mM lactic acid (Sigma) at a density of 1.25×10^6 per dish or 2.5×10^5 per well. Alternatively, neurons were treated at DIV2 with carbonyl cyanide m-chlorophenyl hydrazone (CCCP, Sigma) at a 1.5 µM final concentration, or with the vehicle MeOH (Sigma) at equivalent dilution, for 24h.

Immunocytochemistry. Primary cortical neurons cultured on glass coverslips were fixed with PBS containing 3.7% formaldehyde for 20 min at 37°C. They were permeabilized for 15 min in a PBS solution containing 0.3% Triton X-100 and 10% normal goat serum. Unless otherwise stated, the following incubations and rinsing steps were done in PBS supplemented with 10% goat serum, 5% BSA and 0.5% Tween20. The following primary antibodies were used overnight at 4°C: anti-ATP synthase (mouse, 1:500, A21351, Life Technologies) or anti-Map2 (mouse, M3696, 1:1000, Sigma) plus anti-GFP (chicken, 1:500, ab16901, Millipore). Alexa Fluor 594 goat anti-mouse (Invitrogen, A11005) and Alexa Fluor 488 goat anti-chicken (Invitrogen, A11039) were applied (1:1000) for 1 h at room temperature. After a final incubation with 0.25 µg/ml Hoechst in PBS over 5 min, coverslips were rinsed and mounted in Mowiol and stored at 4°C until analysis under a Leica SP5 confocal microscope.

Morphometric analyses on primary cortical neurons. Morphology of primary cortical neurons was analyzed from z-series of 15-20 optical sections at 0.13 µm interval, with either a 40x oil lens or a 63x oil lens, with or without a digital zoom of 5, acquired on a TCS SP5 confocal system (Leica Microsystem). Three-dimensional reconstructions of series of confocal images were conducted using Imaris XT (Bitplane AG) on deconvoluted images (Huygens SVI). Map2-immunostained dendritic length and branching were measured for ten neurons per well using the NeuronJ add-on to the ImageJ software (http://rsbweb.nih.gov/ij/) and digitized images (40x magnification, three wells per treatment per experiment, n = 3 independent experiments). Spines density and mitochondria analysis of GFP-labeled (GFP+) neurons at DIV9 were performed into proximal dendritic segments located at 20µm from the soma, according to the same method as described below for GFP+ adult-born neurons.

Immunoblotting of proteins extracted from primary cortical neurons. Cells were harvested in lysis buffer (50 mM Tris-HCL pH 7.5, 250 mM NaCl, 5 mM EDTA, 5 mM EGTA, 1 mM dithiothreitol, 0.1% Triton X-100, 0.1% SDS, 1% deoxycholate, 1% NP40) and a protease inhibitor cocktail (« Complete » protease inhibitor mixture, Roche). Lysates were sonicated and protein concentration was determined using a Bradford assay. Proteins (50-100 µg) were separated by SDS-PAGE on a 15% polyacrylamide gel, and analyzed by immunoblotting. The following primary antibodies were used: anti-OPA1 (1:300, BD Biosciences), anti-TFAM (rabbit, 1:2000, ab131607, Abcam), anti-TOM20 (rabbit, 1:25000, sc-11415, Santa Cruz Biotechnology, anti-synapsin (mouse, 1:2000, 106 001, Synaptic Systems), anti-actin (mouse, $1:10^5$, MAB1501, Millipore). After 1h incubation with primary antibodies, the following secondary antibodies were applied (1:5000): polyclonal goat anti-mouse (AbCam, ab6789) or anti-rabbit (AbCam, ab6721) IgG conjugated with horseradish peroxidase. After enhanced chemiluminescent detection of HRP-labeled secondary antibodies, scanned photographic films were analyzed using ImageJ software.

Measurement of oxygen consumption of primary cortical neurons. Oxygen consumption rates (OCR) were assayed using the XF24 Extracellular Flux Analyser (Seahorse Bioscience, North Billerica, MA). Primary cortical neurons (3.10^5) were plated on poly-D-Lysine (Sigma Aldrich) coated XF24 microplates, 9 days before OCR measurements. Dual-analyte sensor cartridges were soaked in XF Calibrant Solution (Seahorse Biosciences) in 24-well cell culture microplates overnight at 37°C to hydrate. Approximately 1h prior to experimentation, injection ports on the sensor cartridge were filled

with drugs from XF Cell Mito Stress Test Kit (Seahorse Bioscience): oligomycin (0.6 µM), Carbonyl cyanide 4-(trifluoromethoxy) phenylhydrazone (FCCP) (6 µM) and rotenone (50 nM) with antimycin A (0.182 µM). For oxygen consumption measurement, neuronal growth medium was replaced 1h prior experimentation with incubation media: DMEM (Sigma Aldrich) supplemented with NaCl (143 mM) (Sigma Aldrich), Phenol Red (3 mg/ml) (Sigma Aldrich), glucose (10 mM) (Sigma Aldrich), glutamine (2 mM) (Sigma Aldrich) and pyruvate (2 mM) (Sigma Aldrich) at pH 7.4, and kept at 37°C. The XF24 microplate was then loaded into the Seahorse XF24 analyser following the manufacturer's instructions. All experiments were carried out at 37°C.

Retroviral vectors. Enhanced-GFP, *Neurod1*-expressing Moloney leukemia-derived retroviral vectors (pCMMP-IRES2eGFP-WPRE, pCMMP-*Neurod1*-IRES2eGFP-WPRE,) were produced and titrated as previously described (Roybon et al., 2009). MitoDsRed-expressing Moloney leukemia-derived retroviral vectors were constructed from the pCAG-IRES-MitoDsRed kindly provided by Dr. DC Lie, produced and titrated as previously described (Roybon et al., 2009). The final titer of each retrovirus solution ranged from $0.5x10^9$ to $3x10^9$ TU/ml. The integration of these retroviral vectors into the host genome occurs only during cell division. Thus, the expression of GFP and *Neurod1* transgenes, as well as MitoDsRed, is restricted to cells dividing shortly after viral injection, allowing visualization and birth dating of transduced cells.

Animals and stereotaxic delivery of the retroviral vectors. We used 7-9 month-old APPsw695/PS1dE9 male mice (Jankowsky et al., 2004). Three days prior to virus injection, mice were placed in individual cages containing a running wheel in order to enhance cell division. Mice were anesthetized with a mixture of ketamine and xylazine and injected with 0.5 µl (speed of 0.1 µl/min) of either viral solution bilaterally into the dentate gyrus, according to stereotaxic coordinates (Bregma: antero-posterior -2 mm, lateral ±1.6 mm, dorso-ventral -2.5 mm from skull) as described before (Richetin et al., 2015). In case of dual infection, 0.5 µl of a mix of 1:1 viral preparations were injected. After recovery in a heated chamber, mice were returned to their home cages. All experiments were performed in strict accordance with the recommendations of The European Communities Council Directive (86/609/EEC), The French National Committee (87/848) and the guide for the Care and Use of Laboratory Animals of the National Institutes of Health (NIH publication nu 85–23). Approval for this study was obtained from FRBT-01 Ethical Comity. All efforts were made to improve animals' welfare and minimize animals suffering.

Immunohistochemistry. At different time-points after viral injection, mice were deeply anesthetized and transcardially perfused with 4% paraformaldehyde in 0.1M-phosphate buffer. Series of 1-in-3, 50µm thick coronal sections were treated 30 min in Dent's 50 (50%DMSO+50%methanol), followed by 30 min in Dent's 25 (25% DMSO+75% methanol), and 10 min in methanol. Then, sections were rinsed in PBST and incubated in a solution of rabbit anti-GFP (1:500, Torrey Pines), mouse anti-OXPHOS (an antibody cocktail directed against representative proteins of each of the 5 complexes of the mitochondrial respiratory chain, 1:100, Abcam) for 48h at 4°C. After several rinses in PBST, sections were incubated for 90 min at room temperature in a solution of Alexa 488-conjugated donkey anti-rabbit (1:500; Life Technologies) and Alexa 555-conjugated donkey anti-mouse (1:500; Life Technologies) in PBST. Sections were rinsed intensively and mounted onto slides, coverslipped using Mowiol and stored at 4°C. Sections surrounding the injection site and displaying signs of lesion were discarded.

Three-dimensional analyses of adult-born neurons. At 14 and 21 dpi, 5-10 GFP+ neurons per mouse were analyzed by acquisition of z-series of 50-75 optical sections at 0.5 µm intervals, with a 40x oil lens, a digital zoom of 1.7, with a TCS SP5 (Leica Microsystem) confocal system. Three-dimensional reconstructions of series of confocal images were conducted using Imaris XT (Bitplane AG) on deconvoluted images (Huygens SVI). Total dendritic length and number of dendritic branching were automatically calculated from three-dimensional reconstructions as described before (Richetin et al., 2015).

Dendritic spine analyses of adult-born neurons. Analysis of dendritic spines on GFP+ neurons was performed on portions of dendrites located after the second branching point by acquiring z-series of 30–50 optical sections at 0.13 µm intervals, with a 63x oil lens, digital zoom of 5, with a TCS SP5 (Leica Microsystem) confocal system. Before analysis, 12-bit files were subjected to seven iterations of deconvolution with the Huygens Essential deconvolution software (SVI). Confocal images were imported into Imaris XT (Bitplane AG) for analysis. Using Imaris surface tracking, the head volume of 50-75 spines per mouse was measured. Dendritic spines were classified on the basis of their shape into four types: filopodia (protrusion with long neck and no head), thin (protrusion with a neck and head <0.6 µm in diameter), stubby (protrusion with no obvious neck or head) or mushroom (protrusion with a neck and a head with a diameter >0.6 µm). For each mouse, 15 dendritic segments were analyzed, corresponding approximately to 1000 µm of dendritic length by group (n=3-5 mice).

Analyses of mitochondria. Analysis of mitochondria located into the soma or distal dendritic segments of GFP+ neurons was performed by acquiring z-series of 100–150 optical sections at 0.13 µm intervals, with a 63x oil lens, a digital zoom of 5, with a TCS SP5 (Leica Microsystem) confocal system. Before analysis, 12-bit files were subjected to seven iterations of deconvolution with the Huygens Essential deconvolution software (SVI). Confocal images were imported into Imaris XT (Bitplane AG) for analysis. The volume of each mitochondria, located inside GFP-labeled compartments, was determined using autoregressive algorithms. Mitochondria were manually excluded from counting if at least 50% of their volume was not included in the GFP-labeled element, by an experimenter blind to the experimental conditions. The mitochondrial biomass index was calculated by dividing the total volume of mitochondria by the GFP volume, for each cellular compartment (soma, dendrite) and expressed as a percentage. Segments were analyzed when located between the beginning of the middle molecular layer and the end of the outer molecular layer. For each time-point (14 and 21 dpi), 5-10 neurons per mice were analyzed (n=3-5 mice / group). Spines with heads were considered to be endowed with mitochondria when one or more mitochondria was found within a maximal distance of 1µm from the basis of the spine neck, as measured with Imaris XT software.

Statistical analysis. For all analyses, the observer was blind to the identity of the samples. Statistical analyses were run with Prism software (GraphPad 5.0). For *in vitro* experiments, Kolmogorov-Smirnov tests were first performed on each data set to test for distribution normality, which led to parametric Student's t-test for data containing less than two experimental conditions, and to the two-way ANOVA test for data containing more than two experimental conditions (Seahorse). For *in vivo* analysis, Shapiro-Wilk tests were first performed on each data set to test for distribution normality and data were analyzed using the one-way ANOVA test.

Experimental design. For all analyses, the observer was blind to the identity of the samples. Samples were coded by a third party and code was broken after analysis was achieved. Animals were randomly assigned to experimental groups.

Results

Neurod1 overexpression in primary neurons enhances neuronal maturation and mitochondrial biomass.

In order to decipher the consequences of *Neurod1* overexpression on the mitochondrial system in maturing neurons, we used primary cortical neurons that represent a highly reliable *in vitro* model to study relationships between neuronal maturation and mitochondrial parameters, as, among others, we previously established (Bertholet et al., 2013). Upon transfection of GFP alone (control, *IRES2-GFP*) or with *Neurod1* (*Neurod1-IRES2-GFP*), we assessed neuronal growth, mitochondrial biomass, number and morphology of mitochondria, as well as expression of neuronal and mitochondrial proteins, at different time-points post-transfection.

Morphometric analysis of transfected neurons revealed significant increases in total dendritic length (Figs. 1a,b) in the presence of *Neurod1* compared with the control group at all time-points (days in vitro (DIV) 3, 6, 9) studied. Moreover, *Neurod1* overexpression significantly increased spinogenesis at DIV9 (Figs. 1c,d). Interestingly, this effect was accompanied by a specific augmentation of the number of mushroom and filopodia spines (Figs. 1c,e). Western blot analyses showed a 60% increase in the neuronal quantity of the pre-synaptic protein synapsin (Fig. 1f), suggesting a concomitant enhancement of pre-synaptic function to establish functional connections.

The impact of *Neurod1* overexpression on neuronal mitochondria was evaluated by fluorescent microscopy after immuno-detection of mitochondrial ATP synthase in GFP-labeled primary neurons at DIV9 (Fig. 2A). Intriguingly, *Neurod1* overexpression led to an increased mitochondrial biomass (calculated by dividing the total volume of mitochondria by the dendrite GFP volume) in the dendritic compartment (Figs. 2a,b). While the number of mitochondria remained unchanged by this treatment (Fig. 2c), their individual volume was significantly increased (Fig. 2d). Our data suggest that the augmentation may be related to an increase in mitochondrial length, since neither their height nor width was modified by *Neurod1* overexpression (Figs. 2e, f).

Further demonstrating the increase in mitochondrial biomass in *Neurod1*-transfected neurons, Western blot analysis showed an approximate 20% elevation in the quantities of two mitochondrial proteins, TOM20 (Fig. 2g) and OPA1 (Fig. 2h), located on the outer and inner mitochondrial membranes respectively, as compared to actin. Similarly, the expression level of the mitochondrial transcriptional regulator TFAM, known to stimulate mitochondrial biogenesis (Scarpulla, 2008), was also increased by over 40% in these neurons (Fig. 2i). We next determined whether such an increase of mitochondrial

biomass accompanied an enhanced mitochondrial function.

Neurod1 overexpression increases mitochondrial respiration

Mitochondrial respiratory chain activity was next investigated by measuring the oxygen consumption rate (OCR) of primary cortical neurons using a Seahorse analyser. In control neurons as well as in *Neurod1*-overexpressing neurons, treatment with rotenone, for the inhibition of complex I, and antimycin A, for the inhibition of complex III, considerably lowered OCR, indicating that over 95% of oxygen consumption was due to mitochondrial respiration (Fig. 3). We used oligomycin, a lipophilic inhibitor of ATP synthase, and Carbonyl cyanide-4-(trifluoromethoxy) phenylhydrazone, FCCP, a well-known uncoupling agent that induces maximal respiration, to quantify the contribution of ATP synthesis to oxygen consumption (Yoboue et al., 2012). In both control and *Neurod1*-overexpressing neurons, application of oligomycin inhibited ATP-linked respiration, while addition of the protonophore FCCP resulted in maximal OCR that was not significantly higher than its spontaneous levels (Fig. 3). This result indicates that in control and *Neurod1*-overexpressing neurons, electron flux through the mitochondrial respiratory chain and ATP generation are coupled, and that spontaneous respiration is close to being maximal. Interestingly, in *Neurod1*-overexpressing neurons, spontaneous and maximal respiration rates are increased compared with control neurons (Fig. 3, Supplementary Fig. 1). Consequently, our results show that *Neurod1* overexpression up-regulates mitochondrial respiration in primary neurons, potentially through an increase of mitochondrial biomass. In an attempt to link the action of *Neurod1* on mitochondria with its beneficial effects on neuronal maturation, we next evaluated the consequences of altering mitochondrial function.

Functional mitochondria are required for the *Neurod1* effect on dendritic growth.

To determine whether the effect of *Neurod1* depends on functional mitochondria, neurons were treated with the protonophore carbonyl cyanide m-chlorophenyl hydrazone (CCCP) to uncouple mitochondrial oxidation and phosphorylation and reduce mitochondrial membrane potential. Thus, we analyzed dendritic length at DIV3 (after Map2 immunostaining) of control GFP and GFP-*Neurod1*-transfected neurons in CCCP and control (vehicle) conditions (Fig. 4). While CCCP treatment had no effect on the dendritic length of control neurons, this condition prevented *Neurod1*-induced increase of dendritic

length (Figs. 4 a,b). This suggests that functional mitochondria are required for the beneficial effect of *Neurod1* on dendritic growth. Altogether, our results indicate that the effects of *Neurod1* overexpression on neuronal maturation are linked to the enhancement of mitochondrial system, and particularly to the increase in respiratory chain activity associated with the augmentation in mitochondrial biomass. Whether *Neurod1* action on adult-generated hippocampal neurons of APPxPS1 mice involved mitochondria was determined next.

Neurod1 **overexpression rescues mitochondrial biogenesis in adult-born hippocampal neurons of APPxPS1 mice.**

Adult-generated hippocampal neurons from APPxPS1 mice display impaired morphology, in particular a lower dendritic spine density that likely contributes to their reduced integration into hippocampal circuits and survival ((Richetin et al., 2015); Supplementary Fig. 2). Virally directed expression of *Neurod1* in cycling hippocampal progenitors conspicuously reduced dendritic spine density deficits of new hippocampal neurons, regardless of the gender of the animals (in females (Richetin et al., 2015)) ; in males, Supplementary Fig. 2). Remarkably, this population of highly connected new neurons was sufficient to restore spatial memory in these diseased mice (Richetin et al., 2015).

In the present work, we examined whether mitochondrial impairment accompanies the morphological alterations of new neurons in AD mice. Because *Neurod1* overexpression in new neurons stimulates spinogenesis in AD mice (Supplementary Fig. 2), we further tested the hypothesis that these *Neurod1*-induced synaptic changes may be related to modifications of the mitochondriome. We thus investigated the mitochondrial content of GFP-labeled adult-born neurons of APPxPS1 mice and non-transgenic (NTg) littermates by mitochondrial immunostaining with a well characterized OXPHOS antibody (Mils et al., 2015). Oxphos immunohistochemistry was found to detect mitochondria in new neurons of mice from both genotypes similarly to MitoDsred retroviral expression (Supplementary Fig 3). As mitochondrial biogenesis occurs in the soma and as mitochondria are distributed further to the proximal and distal dendrites (Fig. 5a), mitochondrial content was determined on 3-D reconstructed images in both the somatic and dendritic compartments (Figs. 5b-e).

We observed that the mitochondrial biomass index (calculated by dividing the total volume of mitochondria by the corresponding cellular GFP volume) was significantly reduced in the somas of 14 day-old adult-born neurons of APPxPS1 compared with NTg mice (Fig. 5c). This effect was mainly

supported by a reduced number of mitochondria located within the somas (Fig. 5d). One week later, at 21 dpi, when new neurons have started to grow dendritic spines (Zhao et al., 2006), the somatic mitochondrial biomass remained significantly reduced in APPxPS1 compared with NTg mice (Fig. 5c). At this time-point, the number of mitochondria was decreased in AD mice, without being significantly different from NTg (Fig. 5d). In the dendritic compartment, the mitochondrial biomass index was identical between genotypes before spinogenesis at 14 dpi (Fig. 5f), but dropped significantly in APPxPS1 mice at 21 dpi compared with NTg after dendritic spine growth, (Fig. 5f). However, the number of mitochondria was similar across genotypes (Fig. 5g), indicating that the decreased mitochondrial biomass in APPxPS1 adult-born neurons was likely attributable to the observed reduction of individual mitochondrial mean volume (NTg injected with control retrovirus, NTg-R-GFP: 0.066±0.016 µm^3 *vs* Tg injected with control retrovirus, APPxPS1-R-GFP: 0.024±0.006 µm^3; P<0.01, data not shown). Altogether, these results raise the possibility that impaired mitochondrial system could contribute to the AD-associated adult neurogenesis defects.

Remarkably, the somatic mitochondrial biomass of APPxPS1 new neurons was rescued upon targeted overexpression of *Neurod1* in the dentate gyrus (Figs. 5b,c). This effect was mainly supported by an enhancement of the number of mitochondria per soma (Fig. 5d). In the dendrites of APPxPS1 new neurons, *Neurod1* overexpression resulted in a significant increase of mitochondrial biomass at 21 dpi, while no change was detected at 14 dpi (Figs. 5e,f), primarily supported by an enhanced number of mitochondria (Fig. 5g) because their individual volume remained stable (APPxPS1-R-GFP: 0.024±0.005 µm^3 *vs* APPxPS1-R-*Neurod1*: 0.032±0.002 µm^3; P>0.05 data not shown).

In summary, *Neurod1* overexpression restores control levels of mitochondrial biomass in adult-generated hippocampal neurons of AD mice. Thus, the rescuing effect of *Neurod1* overexpression on their integration into hippocampal circuits could rely upon the recovery of their mitochondrial content. The parallel rescue of spine equipment and mitochondrial content upon *Neurod1* overexpression led us to further analyze the distribution of mitochondria relative to spines.

Neurod1 overexpression increases the proportion of spines endowed with mitochondria.

Mitochondria have been shown to be distributed all along the dendritic arbor and to be occasionally associated with dendritic spines of mature neurons (Cameron et al., 1991; Popov et al., 2005). The distribution of mitochondria relative to spines in the dendrites of adult-born neurons remained to be established.

In NTg mice, we found that dendritic spines contained small mitochondria that were mainly localized into the dendritic shaft. This distribution is also observed in APPxPS1 new neurons, which noticeably contain fewer dendritic spines than NTg new neurons (Supplementary Figs. 2c,d), regardless of their shape, i.e. filopodia, stubby, thin and mushroom spines (Harris and Stevens, 1989), (Fig. 6a). Interestingly, the beneficial effect of *Neurod1* on spinogenesis in adult-born neurons of APPxPS1 mice, which was distributed across all types of spines (Supplementary Figs 2c,d; Fig. 6a), correlated with an increased proportion of spines closely associated with mitochondria (Fig. 6b) in comparable proportions in stubby, thin and mushroom subtypes (Fig. 6c).

Altogether, our results suggest that the enhancing effect of *Neurod1* overexpression in adult-born neurons of APPxPS1 mice on their mitochondrial equipment is likely to support its concomitant stimulating action on their morphological maturation. Moreover, our data lead to the idea that the rescue of new neurons connectivity in AD mice upon *Neurod1* overexpression involves an increase of functional synapses that could involve the recruitment of mitochondria in the close vicinity of spines.

Discussion

The production of new neurons in the adult mammalian brain throughout adult life has been shown to foster cognitive and memory functions (Aimone et al., 2011; Kim et al., 2012). The addition of functional adult-born granule cells into the hippocampal network provides a unique form of plasticity critically underlying learning and memory processes. However, in several mouse models of Alzheimer's disease, hippocampal adult neurogenesis is impaired and the granule neurons that are generated fail to integrate into existing networks, thus contributing to spatial memory deficits (Mu and Gage, 2011; Richetin et al., 2015). In this study, we provide the first evidence that impaired morphological development and integration of hippocampal adult-born neurons in the AD brain is associated with a reduction of their mitochondrial biomass. Using a gene-targeting strategy to deliver the bHLH transcription factor *Neurod1* selectively into dividing neural stem cells of the adult hippocampus *in vivo*, we promoted their differentiation into neurons, and subsequent integration into the hippocampal circuit, together with an enhancement of their mitochondrial content and respiratory function, and an increase of mitochondrial association to dendritic spines. Moreover, we demonstrated that the beneficial effects of *Neurod1* on neuronal morphology could not occur under limited mitochondrial function, suggesting a causal relationship between these two events.

Functional mitochondria condition *Neurod1* effect on dendritic growth

Mitochondria are critical elements regulating many biological processes such as energy production, calcium homeostasis and ROS generation. As cellular hubs, mitochondria adapt to environmental changes through biogenesis and degradation processes and dynamic shape modifications (Nunnari and Suomalainen, 2012). Indicative of the crucial role of this organelle, manipulation of the mitochondrial components are thought to affect the pluripotency of embryonic stem cells (Chen et al., 2012). The developmental sequence leading to the production of functional neurons from quiescent neural stem cells is a major challenge for mitochondria, and is associated with an upregulation of mitochondrial function and antioxidant defenses (Chen et al., 2010; Cordeau-Lossouarn et al., 1991). Moreover, *in vitro* neuritogenesis is associated with mitochondrial accumulation in growth cones (Morris and Hollenbeck, 1995, 1993), and is related *in vivo*, together with synaptogenesis, to augmentations in mitochondrial number, volume and cristae (Erecinska et al., 2004). Thus, neuronal maturation seems linked to mitochondrial biogenesis and is also characterized by changes in mitochondrial shape (Bertholet et al., 2013; Mils et al., 2015). These events are evocative of a metabolic shift from glycolysis to oxidative phosphorylation, allowing mitochondria to become highly efficient providers of ATP able to fulfill high energy demands. Reciprocally, impairment of mitochondrial ATP production leads to dendritic growth defects indicating that mitochondria-dependent energy production is required for dendritogenesis (Oruganty-Das et al., 2012). Moreover, mitochondria-dependent Ca2+ buffering influences the development of neuronal morphology *in vitro* (Dickey and Strack, 2011; MacAskill et al., 2010). Furthermore, several *in vitro* studies have shown that disruption of proteins key to mitochondrial dynamics is sufficient to affect dendritogenesis and synaptogenesis (Bertholet et al., 2013; Li et al., 2004; Steketee et al., 2012).

Neurod1 exerts neurogenic and neurotrophic effects on hippocampal neural stem cells *in vivo* (Richetin et al., 2015), and by itself, directs exclusive neuronal differentiation and maturation of cortico-hippocampal-derived progenitors *in vitro* and *in* vivo (Roybon et al., 2009). We have previously shown that two weeks after injection of the control-GFP virus, GFP+ cells were identified to be also positive for the neural stem cell markers such as PAX6, MASH1 and proliferation marker Ki67 indicating that very early developmental stages are targeted. Moreover, when the Neurod1 virus was injected, none of the GFP+ cells was found positive for these markers (Roybon et al. 2009) indicating that Neurod1 directs exclusive and rapid neuronal differentiation of targeted neural stem cells. We thus

overexpressed *Neurod1* in primary neurons and interrogated the possible involvement of mitochondria in *Neurod1* neurotrophic effects. Here, we confirmed that *Neurod1* overexpression increases dendritic growth and spinogenesis during neuronal maturation. Simultaneously, we observed an augmentation of mitochondrial biomass and respiration, suggesting that *Neurod1* overexpression stimulates mitochondrial biogenesis *in vitro*. This result is in line with seminal studies demonstrating that neuronal differentiation is chloramphenicol-sensitive, thus dependent on mitochondrial protein synthesis (Vayssière et al., 2016). In order to identify a causal link between this mitochondrial amplification and dendritogenesis, we identified a CCCP dose for which a short-term treatment had no consequence on dendritic growth nor viability of control neurons. Remarkably, when this CCCP treatment is applied to *Neurod1*-overexpressing neurons exhibiting increased mitochondrial content and higher mitochondrial respiration, further *Neurod1*-promoting effects on dendritic growth are abolished *in vitro*. This strongly suggests that *Neurod1*-induced dendritic growth depends on mitochondrial respiration coupling to oxidative phosphorylation, thus, potentially, on the synthesis of mitochondrial ATP. Similarly, synchronization between enhanced mitochondrial respiratory chain activity and neurite outgrowth was reported in immortalized hippocampal neuroblasts (Voccoli and Colombaioni, 2009). Interestingly, local NGF application triggered mitochondrial respiration in axons of cultured embryonic chick sensory neurons, further stressing the role played by mitochondrial respiration in neuritogenesis (Verburg and Hollenbeck, 2008).

In the same way, another member of the NeuroD family, *Neurod6*, was demonstrated *in vitro* to play an integrative role in coordinating an increase of mitochondrial biomass with cytoskeletal remodeling, suggesting a role for *Neurod6* as a co-regulator of neuronal differentiation and energy metabolism (Baxter et al., 2009). Overexpression of *NeuroD6* was further shown to enhance antioxidant mechanisms through the action of ROS-scavenging enzymes on the one hand, but also to induce key actors of mitochondrial biogenesis, turn-over and functioning such as PGC-1-alpha, PINK1 and SIRT1 on the other hand (Uittenbogaard et al., 2010). These data point to a specific transcriptional program that involves NeuroD members and sustains the maintenance and integrity of mitochondrial biomass in order to mediate neuronal growth and survival.

It is known that members of the bHLH NeuroD family are essential for terminal neuronal differentiation during neurogenesis (Guillemot, 2007), a time when total mitochondrial protein content increases (Cordeau-Lossouarn et al., 1991). *Neurod1* expression peaks in late stage type 2b and type 3 cells and then decreases during granule neuron maturation (Gao et al., 2009; Roybon et al., 2009). *Neurod1* is also required for the survival of adult-born neurons in the adult dentate gyrus (Miyata et al.,

1999), raising the question of the nature of its molecular targets. Very recently, a thorough transcriptomic analysis showed that *Neurod1* directly binds regulatory elements of key neuronal development genes (Pataskar et al., 2016). Even indirectly triggered by *Neurod1*, the mitochondrial biomass increase confirms the involvement of mitochondrial biogenesis in the plasticity of neuronal circuits through the establishment and maintenance of dendritic spines, further supported by previous reports. Indeed, it was shown that knockdown experiments of the master regulator of this process, PGC-1alpha, both in primary and adult mouse hippocampal neurons, lead to the inhibition of spinogenesis and synaptogenesis (Cheng et al., 2012).

Adult-generated hippocampal neurons of APPxPS1 mice exhibit altered mitochondrial content.

It is well established that mitochondrial dysfunction is intimately linked to the pathophysiology of aging and neurodegeneration (Bratic and Larsson, 2013), including AD. In the APPxPS1 mouse model of AD at 3 and 6 months of age a reduction of mitochondrial biogenesis factors NRF1 and PGC-1alpha was reported (Pedrós et al., 2014). More specifically, *in vitro* investigations on primary neurons have revealed that exposure to the amyloid beta peptide led to mitochondrial perturbations, including reduced membrane potential, increased permeability, increased ROS production, altered trafficking, and aberrant mitochondrial shaping (Manczak et al., 2011, 2006; Reddy, 2009; Wang et al., 2008). Impaired neuronal connectivity in the AD context was further evidenced by loss of synaptic mitochondria integrity and energy production in primary hippocampal and cortical neurons of AD mouse models, including the APPxPS1 mice (Trushina et al., 2012). Similarly, in several mouse models of AD, hippocampal adult neurogenesis is impaired and the granule neurons that are generated fail to integrate existing networks, likely contributing to spatial memory deficits (Krezymon et al., 2013; Verret et al., 2007). Based on these data, we hypothesized that mitochondrial availability could influence the integration of new hippocampal neurons through their capacity to form and stabilize dendritic synapses, a process particularly challenged in the AD brain. Supporting this hypothesis, we provide the first evidence that the mitochondrial biomass is drastically reduced both in the soma and dendrites of adult-born hippocampal neurons of APPxPS1 mice.

Neurod1 rescues mitochondrial biomass and spinogenesis in APPxPS1 mice adult-born neurons.

Because we recently reported that the delivery of *Neurod1* into cycling hippocampal progenitors conspicuously restores the production of functional neurons in AD mice model, which, in turn, abolishes spatial memory deficits (Richetin et al., 2015), we investigated the consequences of *Neurod1* expression in neural progenitors on the mitochondrial content of newly-generated hippocampal neurons. We show that overexpressing *Neurod1* in adult-born neurons of APPxPS1 mice increased their mitochondrial biomass, as observed in wild-type primarily cultured neurons, suggesting a cell-autonomous effect. Thus, our data indicate that manipulating the mitochondrial system through the expression of *Neurod1* promotes spinogenesis and mitochondrial availability at the vicinity of mature spines. Mechanistically, this mitochondrial targeting to spines could reflect newly formed active synapses, possibly because of Ca2+ entry through ionotropic glutamate receptors, shown to regulate mitochondrial trafficking (MacAskill et al., 2010). As a result, Neurod1 expression is likely to improve the integration and survival of adult-generated hippocampal neurons, impaired in AD mouse models.

Until recently, the contribution of mitochondria to the development of new neurons in the adult brain had remained unexplored. The seminal work by Lie's group showed that the regulation of mitochondrial dynamics, which controls mitochondrial shaping by fusion and fission events, is part of the developmental program that supervises the generation of new neurons during adulthood (Steib et al., 2014). More recently, the fission protein DRP1 was shown to control the migration and neuronal differentiation of the subventricular zone-derived neural progenitor cells (Kim et al., 2015). Clearly, mitochondria appear to specifically contribute to the establishment of synaptic function at the spine level, as supported by the negative consequences of mitochondrial content reduction (by knockdown of PGC-1alpha) that is observed on dendritic spine formation in cultured hippocampal neurons (Cheng et al., 2012). Very recently, an elegant study confirmed that mitochondrial complex function defines a critical developmental step in adult hippocampal neurogenesis (Beckervordersandforth et al., 2017). This work further suggests that manipulating mitochondrial function in adult-born neurons may be used to develop novel therapeutic strategies against pathologies associated with neurogenesis alterations. In the present work, we provide the first evidence that this could be the case in Alzheimer's disease.

Overall, our work sustains the hypothesis that the failure of adult-born neurons to achieve their functional integration in the AD brain could be linked to mitochondrial defects. As such, our findings bring new light to a supplementary consequence of mitochondrial defects in the pathophysiology of

aging and neurodegeneration (Beckervordersandforth et al., 2017, Bertholet et al., 2016; Bratic and Larsson, 2013; Schon and Przedborski, 2011). Importantly, our data brings promising evidence that in a diseased brain, manipulations of mitochondrial biogenesis designed to enhance mitochondrial function could be a trigger to sustain functional integration of adult-born neurons, a process that supports memory function.

Acknowledgements

We warmly thank Dr. L. Mouledous, S. Pech, H. Halley and B. Ronsin at Toulouse University 3 for their technical support. We thank Dr. M. Dhenain for his precious help. We acknowledge the ABC facility from ANEXPLO Toulouse for housing mice and Toulouse Réseau Imagerie, FRBT-CBI for the microscopic platform. We also thank Drs. D. Arvanitis and V. Setola for their critical reading of the manuscript and helpful comments.

Funding

This work was supported by grants from the Fondation pour la Recherche sur le Cerveau (FRC), JPND EU MADGIC program and the Association France Alzheimer to C.R., by the CNRS and Toulouse University. K.R. was supported by a fellowship from the French Ministry for Research, M.M. was supported by a fellowship from “Gueules cassées sourire quand même”, T.A. was supported by a fellowship from the Ministry of Research, Technology and Higher Education Republic of Indonesia, M.S.A. was supported by a fellowship from Chile CONACYT.

Authors contributions

KR, CR and MCM designed the study and wrote the manuscript. KR carried out the *in vivo* experiments and analyzed the data. MM, PB, TA, MSA and JH designed, performed and analyzed the *in vitro* experiments. AM and ND designed, performed and analyzed the SeaHorse experiments. LR designed and produced the retroviral vectors. All authors revised and discussed the manuscript, and approved its final version.

Competing financial interests

The authors declare no conflict of interest.

References

Aimone, J.B., Deng, W., Gage, F.H., 2011. Resolving New Memories: A Critical Look at the Dentate Gyrus, Adult Neurogenesis, and Pattern Separation. Neuron 70, 589–596. doi:10.1016/j.neuron.2011.05.010

Altman, J., Das, G.D., 1965. Autoradiographic and histological evidence of postnatal hippocampal neurogenesis in rats. J Comp Neurol 124, 319–335.

Baxter, K.K., Uittenbogaard, M., Yoon, J., Anne. Chiaramello, Kathleen Baxter, K., Chiaramello, A., Kristin.Uittenbogaard, Martine, 2009. The neurogenic basic helix-loop-helix transcription factor NeuroD6 concomitantly increases mitochondrial mass and regulates cytoskeletal organization in the early stages of neuronal differentiation. ASN Neuro 1. doi:10.1042/AN20090036

Beckervordersandforth, R., Ebert, B., Sch, I., Jessberger, S., Song, H., Moss, J., Fiebig, C., Shin, J., 2017. Role of Mitochondrial Metabolism in the Control of Early Lineage Progression and Aging Phenotypes in Adult Hippocampal Neurogenesis 1–14. doi:10.1016/j.neuron.2016.12.017

Bertholet, A.M., Delerue, T., Millet, A.M., Moulis, M.F., David, C., Daloyau, M., Arnauné-Pelloquin, L., Davezac, N., Mils, V., Miquel, M.C., Rojo, M., Belenguer, P., 2016. Mitochondrial fusion/fission dynamics in neurodegeneration and neuronal plasticity. Neurobiol. Dis. 90, 3–19. doi:10.1016/j.nbd.2015.10.011

Bertholet, A.M., Millet, A.M.E., Guillermin, O., Daloyau, M., Davezac, N., Miquel, M.-C., Belenguer, P., 2013. OPA1 loss of function affects in vitro neuronal maturation. Brain 136, 1518–33. doi:10.1093/brain/awt060

Bratic, A., Larsson, N.-G., 2013. The role of mitochondria in aging. J. Clin. Invest. 123, 951–7. doi:10.1172/JCI64125

Cameron, H.A., Kaliszewski, C.K., Greer, C.A., 1991. Organization of mitochondria in olfactory bulb granule cell dendritic spines. Synapse 8, 107–18. doi:10.1002/syn.890080205

Chen, C.-T., Hsu, S.-H., Wei, Y.-H., 2012. Mitochondrial bioenergetic function and metabolic plasticity in stem cell differentiation and cellular reprogramming. Biochim. Biophys. Acta 1820, 571–6. doi:10.1016/j.bbagen.2011.09.013

Chen, H., Vermulst, M., Wang, Y.E., Chomyn, A., Prolla, T.A., McCaffery, J.M., Chan, D.C., 2010. Mitochondrial fusion is required for mtDNA stability in skeletal muscle and tolerance of mtDNA mutations. Cell 141, 280–9. doi:10.1016/j.cell.2010.02.026

Cheng, A., Hou, Y., Mattson, M.P., 2010. Mitochondria and neuroplasticity. ASN Neuro 2, e00045. doi:10.1042/AN20100019

Cheng, A., Wan, R., Yang, J.-L., Kamimura, N., Son, T.G., Ouyang, X., Luo, Y., Okun, E., Mattson, M.P., 2012. Involvement of PGC-1α in the formation and maintenance of neuronal dendritic spines. Nat. Commun. 3, 1250. doi:10.1038/ncomms2238

Cordeau-Lossouarn, L., Vayssière, J.L., Larcher, J.C., Gros, F., Croizat, B., 1991. Mitochondrial maturation during neuronal differentiation in vivo and in vitro. Biol. Cell 71, 57–65.

Demars, M., Hu, Y.-S., Gadadhar, A., Lazarov, O., 2010. Impaired neurogenesis is an early event in the etiology of familial Alzheimer's disease in transgenic mice. J. Neurosci. Res. 88, 2103–17. doi:10.1002/jnr.22387

Dickey, A.S., Strack, S., 2011. PKA/AKAP1 and PP2A/Bβ2 regulate neuronal morphogenesis via Drp1 phosphorylation and mitochondrial bioenergetics. J. Neurosci. 31, 15716–26. doi:10.1523/JNEUROSCI.3159-11.2011

Erecinska, M., Cherian, S., Silver, I.A., 2004. Energy metabolism in mammalian brain during development. Prog. Neurobiol. 73, 397–445. doi:10.1016/j.pneurobio.2004.06.003

Eriksson, P.S., Perfilieva, E., Bjork-Eriksson, T., Alborn, A.M., Nordborg, C., Peterson, D.A., Gage, F.H., 1998. Neurogenesis in the adult human hippocampus. Nat Med 4, 1313–1317. doi:10.1038/3305

Gao, Z., Ure, K., Ables, J.L., Lagace, D.C., Nave, K.A., Goebbels, S., Eisch, A.J., Hsieh, J., 2009. Neurod1 is essential for the survival and maturation of adult-born neurons. Nat Neurosci 12, 1090–1092. doi:10.1038/nn.2385

Gu, Y., Arruda-Carvalho, M., Wang, J., Janoschka, S.R., Josselyn, S. a, Frankland, P.W., Ge, S., 2012. Optical controlling reveals time-dependent roles for adult-born dentate granule cells. Nat. Neurosci. 15, 1700–6. doi:10.1038/nn.3260

Guillemot, F., 2007. Cell fate specification in the mammalian telencephalon. Prog. Neurobiol. 83, 37–52. doi:10.1016/j.pneurobio.2007.02.009

Hagberg, H., Mallard, C., Rousset, C.I., Thornton, C., 2014. Mitochondria: Hub of injury responses in the developing brain. Lancet Neurol. doi:10.1016/S1474-4422(13)70261-8

Hamilton, A., Holscher, C., 2012. The effect of ageing on neurogenesis and oxidative stress in the APP(swe)/PS1(deltaE9) mouse model of Alzheimer's disease. Brain Res. 1449, 83–93. doi:10.1016/j.brainres.2012.02.015

Harris, K.M., Stevens, J.K., 1989. Dendritic spines of CA 1 pyramidal cells in the rat hippocampus: serial electron microscopy with reference to their biophysical characteristics. J. Neurosci. 9, 2982–2997.

Hirai, K., Aliev, G., Nunomura, A., Fujioka, H., Russell, R.L., Atwood, C.S., Johnson, A.B., Kress, Y.,

Vinters, H. V, Tabaton, M., Shimohama, S., Cash, A.D., Siedlak, S.L., Harris, P.L., Jones, P.K., Petersen, R.B., Perry, G., Smith, M.A., 2001. Mitochondrial abnormalities in Alzheimer's disease. J. Neurosci. 21, 3017–23. doi:21/9/3017 [pii]

Jankowsky, J.L., Fadale, D.J., Anderson, J., Xu, G.M., Gonzales, V., Jenkins, N.A., Copeland, N.G., Lee, M.K., Younkin, L.H., Wagner, S.L., Younkin, S.G., Borchelt, D.R., 2004. Mutant presenilins specifically elevate the levels of the 42 residue beta-amyloid peptide in vivo: evidence for augmentation of a 42-specific gamma secretase. Hum. Mol. Genet. 13, 159–70. doi:10.1093/hmg/ddh019

Kim, H.J., Shaker, M.R., Cho, B., Cho, H.M., Kim, H., Kim, J.Y., Sun, W., 2015. Dynamin-related protein 1 controls the migration and neuronal differentiation of subventricular zone-derived neural progenitor cells. Sci. Rep. 5, 15962. doi:10.1038/srep15962

Kim, W.R., Christian, K., Ming, G.L., Song, H., 2012. Time-dependent involvement of adult-born dentate granule cells in behavior. Behav. Brain Res. doi:10.1016/j.bbr.2011.07.012

Krezymon, A., Richetin, K., Halley, H., Roybon, L., Lassalle, J.M., Francès, B., Verret, L., Rampon, C., 2013. Modifications of Hippocampal Circuits and Early Disruption of Adult Neurogenesis in the Tg2576 Mouse Model of Alzheimer's Disease. PLoS One 8, 9–11. doi:10.1371/journal.pone.0076497

Li, Z., Okamoto, K., Hayashi, Y., Sheng, M., 2004. The Importance of Dendritic Mitochondria in the Morphogenesis and Plasticity of Spines and Synapses. Cell 119, 873–887. doi:10.1016/j.cell.2004.11.003

MacAskill, A.F., Atkin, T.A., Kittler, J.T., 2010. Mitochondrial trafficking and the provision of energy and calcium buffering at excitatory synapses. Eur. J. Neurosci. 32, 231–40. doi:10.1111/j.1460-9568.2010.07345.x

Magnifico, S., Saias, L., Deleglise, B., Duplus, E., Kilinc, D., Miquel, M.-C., Viovy, J.-L., Brugg, B., Peyrin, J.-M., 2013. NAD+ acts on mitochondrial SirT3 to prevent axonal caspase activation and axonal degeneration. FASEB J. 27, 4712–22. doi:10.1096/fj.13-229781

Manczak, M., Anekonda, T.S., Henson, E., Park, B.S., Quinn, J., Reddy, P.H., 2006. Mitochondria are a direct site of A beta accumulation in Alzheimer's disease neurons: implications for free radical generation and oxidative damage in disease progression. Hum. Mol. Genet. 15, 1437–49. doi:10.1093/hmg/ddl066

Manczak, M., Calkins, M.J., Reddy, P.H., 2011. Impaired mitochondrial dynamics and abnormal interaction of amyloid beta with mitochondrial protein Drp1 in neurons from patients with Alzheimer ' s disease : implications for neuronal damage. Hum. Mol. Genet. 20, 2495–2509.

doi:10.1093/hmg/ddr139

Mattson, M.P., 2008. Glutamate and neurotrophic factors in neuronal plasticity and disease. Ann. N. Y. Acad. Sci. 1144, 97–112. doi:10.1196/annals.1418.005

Mils, V., Bosch, S., Roy, J., Bel-Vialar, S., Belenguer, P., Pituello, F., Miquel, M.-C., 2015. Mitochondrial reshaping accompanies neural differentiation in the developing spinal cord. PLoS One 10, e0128130. doi:10.1371/journal.pone.0128130

Miyata, T., Maeda, T., Lee, J.E., 1999. NeuroD is required for differentiation of the granule cells in the cerebellum and hippocampus. Genes Dev 13, 1647–1652.

Morris, R.L., Hollenbeck, P.J., 1995. Axonal transport of mitochondria along microtubules and F-actin in living vertebrate neurons. J. Cell Biol. 131, 1315–26.

Morris, R.L., Hollenbeck, P.J., 1993. The regulation of bidirectional mitochondrial transport is coordinated with axonal outgrowth. J. Cell Sci. 104, 917–927.

Mu, Y., Gage, F.H., 2011. Adult hippocampal neurogenesis and its role in Alzheimer's disease. Mol. Neurodegener. 6, 85. doi:10.1186/1750-1326-6-85

Nunnari, J., Suomalainen, A., 2012. Mitochondria: in sickness and in health. Cell 148, 1145–59. doi:10.1016/j.cell.2012.02.035

Oruganty-Das, A., Ng, T., Udagawa, T., Goh, E.L.K., Richter, J.D., 2012. Translational control of mitochondrial energy production mediates neuron morphogenesis. Cell Metab. 16, 789–800. doi:10.1016/j.cmet.2012.11.002

Pataskar, A., Jung, J., Smialowski, P., Noack, F., Calegari, F., Straub, T., Tiwari, V.K., 2016. NeuroD1 reprograms chromatin and transcription factor landscapes to induce the neuronal program. EMBO J. 35, 24–45. doi:10.15252/embj.201591206

Pedrós, I., Petrov, D., Allgaier, M., Sureda, F., Barroso, E., Beas-Zarate, C., Auladell, C., Pallàs, M., Vázquez-Carrera, M., Casadesús, G., Folch, J., Camins, A., 2014. Early alterations in energy metabolism in the hippocampus of APPswe/PS1dE9 mouse model of Alzheimer's disease. Biochim. Biophys. Acta - Mol. Basis Dis. 1842, 1556–1566. doi:10.1016/j.bbadis.2014.05.025

Popov, V., Medvedev, N.I., Davies, H.A., Stewart, M.G., 2005. Mitochondria form a filamentous reticular network in hippocampal dendrites but are present as discrete bodies in axons: a three-dimensional ultrastructural study. J. Comp. Neurol. 492, 50–65. doi:10.1002/cne.20682

Reddy, P.H., 2009. Role of mitochondria in neurodegenerative diseases: mitochondria as a therapeutic target in Alzheimer's disease. CNS Spectr. 14, 8-13-18.

Richetin, K., Leclerc, C., Toni, N., Gallopin, T., Pech, S., Roybon, L., Rampon, C., 2015. Genetic manipulation of adult-born hippocampal neurons rescues memory in a mouse model of

Alzheimer's disease. Brain 138, 440–455. doi:10.1093/brain/awu354

Roybon, L., Hjalt, T., Stott, S., Guillemot, F., Li, J.Y., Brundin, P., 2009. Neurogenin2 directs granule neuroblast production and amplification while NeuroD1 specifies neuronal fate during hippocampal neurogenesis. PLoS One 4, e4779. doi:10.1371/journal.pone.0004779

Scarpulla, R.C., 2008. Transcriptional paradigms in mammalian mitochondrial biogenesis and function. Physiol. Rev. 88, 611–638. doi:10.1152/physrev.00025.2007

Schon, E.A., Przedborski, S., 2011. Mitochondria: the next (neurode)generation. Neuron 70, 1033–53. doi:10.1016/j.neuron.2011.06.003

Steib, K., Scha, I., Jagasia, R., Ebert, B., Lie, D.C., 2014. Mitochondria Modify Exercise-Induced Development of Stem Cell-Derived Neurons in the Adult Brain. J. Neurosci. 34, 6624–6633. doi:10.1523/JNEUROSCI.4972-13.2014

Steketee, M.B., Moysidis, S.N., Weinstein, J.E., Kreymerman, A., Silva, J.P., Iqbal, S., Goldberg, J.L., 2012. Mitochondrial dynamics regulate growth cone motility, guidance, and neurite growth rate in perinatal retinal ganglion cells in vitro. Invest. Ophthalmol. Vis. Sci. 53, 7402–11. doi:10.1167/iovs.12-10298

Taniuchi, N., Niidome, T., Goto, Y., Akaike, A., Kihara, T., Sugimoto, H., 2007. Decreased proliferation of hippocampal progenitor cells in APPswe/PS1dE9 transgenic mice. Neuroreport 18, 1801–1805. doi:10.1097/WNR.0b013e3282f1c9e9

Trushina, E., Nemutlu, E., Zhang, S., Christensen, T., Camp, J., Mesa, J., Siddiqui, A., Tamura, Y., Sesaki, H., Wengenack, T.M., Dzeja, P.P., Poduslo, J.F., 2012. Defects in mitochondrial dynamics and metabolomic signatures of evolving energetic stress in mouse models of familial alzheimer's disease. PLoS One 7, e32737. doi:10.1371/journal.pone.0032737

Uittenbogaard, M., Baxter, K.K., Chiaramello, A., 2010. The neurogenic basic helix-loop-helix transcription factor NeuroD6 confers tolerance to oxidative stress by triggering an antioxidant response and sustaining the mitochondrial biomass. ASN Neuro 2, e00034. doi:10.1042/AN20100005

Vayssière, J.L., Cordeau-Lossouarn, L., Larcher, J.C., Basseville, M., Gros, F., Croizat, B., 2016. Participation of the mitochondrial genome in the differentiation of neuroblastoma cells. In Vitro Cell. Dev. Biol. 28A, 763–72.

Verburg, J., Hollenbeck, P.J., 2008. Mitochondrial membrane potential in axons increases with local nerve growth factor or semaphorin signaling. J. Neurosci. 28, 8306–15. doi:10.1523/JNEUROSCI.2614-08.2008

Verret, L., Jankowsky, J.L., Xu, G.M., Borchelt, D.R., Rampon, C., 2007. Alzheimer ' s-Type

Amyloidosis in Transgenic Mice Impairs Hippocampal Neurogenesis. Amyloid Int. J. Exp. Clin. Investig. 27, 6771–6780. doi:10.1523/JNEUROSCI.5564-06.2007

Voccoli, V., Colombaioni, L., 2009. Mitochondrial remodeling in differentiating neuroblasts. Brain Res. 1252, 15–29. doi:10.1016/j.brainres.2008.11.026

Vos, M., Lauwers, E., Verstreken, P., 2010. Synaptic mitochondria in synaptic transmission and organization of vesicle pools in health and disease. Front. Synaptic Neurosci. 2, 1–10. doi:10.3389/fnsyn.2010.00139

Wang, X., Su, B., Siedlak, S.L., Moreira, P.I., Fujioka, H., Wang, Y., Casadesus, G., Zhu, X., 2008. Amyloid-beta overproduction causes abnormal mitochondrial dynamics via differential modulation of mitochondrial fission/fusion proteins. Proc. Natl. Acad. Sci. U. S. A. 105, 19318–23. doi:10.1073/pnas.0804871105

Yoboue, E.D., Augier, E., Galinier, A., Blancard, C., Pinson, B., Casteilla, L., Rigoulet, M., Devin, A., 2012. cAMP-induced mitochondrial compartment biogenesis: Role of glutathione redox state. J. Biol. Chem. 287, 14569–14578. doi:10.1074/jbc.M111.302786

Zhao, C., Teng, E.M., Summers Jr, R.G., Ming, G.-L., Gage, F.H., 2006. Distinct Morphological Stages of Dentate Granule Neuron Maturation in the Adult Mouse Hippocampus. J. Neurosci. 26, 3–11. doi:10.1523/JNEUROSCI.3648-05.2006

Figure legends

Figure 1: *Neurod1* overexpression stimulates dendritogenesis and spinogenesis of primary neurons *in vitro*. (a) Representative fluorescence micrograph of GFP (top) and GFP-Neurod1 (bottom) -expressing primary neurons in culture at 3 and 6 days *in vitro* (DIV). A reconstruction of such neuron at DIV9 is also provided (bottom right) **(b)** Histogram representing the total dendritic length of primary neurons at DIV 3, 6 and 9 transfected with vectors expressing GFP alone (GFP) or both GFP and *Neurod1* (*Neurod1*) and showing the growth stimulating effect of *Neurod1* overexpression. Data are expressed as the mean ± SEM, average of 40 neurons, n=3, Student's t-test, *P<0.05, **P<0.01, ***P<0.001 **(c)** High magnifications showing dendrites (top) and spines (bottom) of a DIV9 primary neurons transfected with control or *Neurod1* vectors (Scale bars = 10µm; 1 µm). Data are expressed as mean ± SEM, n=3; Student's t-test, ***P < 0.001. Effects of *Neurod1* overexpression on **(d)** total spine density and **(e)** individual spine subtypes of DIV 9 primary neurons transfected with control or *Neurod1* vectors. **(f)** Expression of a presynaptic protein synapsin relative to actin levels and normalized to control values (AU = arbitrary units). Neurons overexpressing *Neurod1* exhibit more spines, specifically of mushroom and filopodia subtypes, than control neurons. Data are expressed as the mean ± SEM, n=3; Student's t-test **P < 0.05.

Figure 2: *Neurod1* overexpression increases mitochondrial biomass and length of neurons in vitro. (a) Representative fluorescence micrographs (bottom left) and 3D reconstruction (top left and right) of dendritic segments of DIV9 neurons immunostained for GFP (green) and ATPase (red) (Bars = 8µm and 2µm, respectively). **(b-d)** Histograms illustrating the volume occupied by mitochondria per GFP volume (**b**), the number (**c**) and individual volume (**d**) of mitochondria in control (GFP) or *Neurod1* conditions. At DIV 9, overexpression of *Neurod1* increased the mitochondrial content in GFP+ dendritic segments and the individual mitochondrial volume. Data represent the mean ± SEM, average of 40 neurons, n=3, Student's t-test, *P<0.05, ***P<0.001. **(e)** For each mitochondrion in control and *Neurod1* conditions, the length of the 3 ellipsoid axes was estimated from 3D images. (**f**) Graph illustrating the influence of *Neurod1* overexpression on mitochondria ellipsoid shape. Overexpression of *Neurod1* increased mitochondria length but had no major effect on their height and width. Data correspond to the mean ± SEM, average of 40 neurons, n=3, Student's t-test, ***P<0.001. **(g-i)** Histograms and representative blots depicting the influence of *Neurod1* overexpression on the expression of the mitochondrial proteins TOM20 (**g**), OPA1 (**h**) and TFAM (**i**) relative to actin and

normalized to control values (Data are expressed in AU= arbitrary units, and represent the mean ± SEM, n=5, Student's t-test *P<0.05).

Figure 3. *Neurod1* overexpression stimulates spontaneous and maximal mitochondrial respiration. (a) Oxygen consumption rates (OCR) were measured at 9 days *in vitro* (DIV9) in GFP (white squares) or *Neurod1*-overexpressing (black squares) neurons. Spontaneous mitochondrial respiration is significantly increased in *Neurod1*-overexpressing neurons as compared with controls. After 6 µM FCCP injection, maximal respiration is significantly higher in *Neurod1*-overexpressing neurons compared with controls. Finally, 50 nM rotenone (Rot) and 0.18 µM antimycin A (AA) injections inhibit mitochondrial respiration to the same extent in both conditions. Data represent the mean ± SEM, n=4, two-way ANOVA ***P<0.001, ****P<0.0001.

Figure 4: Growth promoting effects of *Neurod1* are prevented by mitochondrial membrane potential impairment. (a) Representative photomicrographs of DIV3 primary neurons (green) transfected with GFP- or GFP-*Neurod1*-expressing vectors at DIV0, after a 24h CCCP (1.5 µM) or vehicle (control) treatment (Scale bar = 50 µm). **(b)** Histograms illustrating the total dendritic length of control (GFP) or *Neurod1* primary neurons under vehicle or CCCP conditions. Transfection with *Neurod1* robustly promotes neuronal dendritic growth, and this effect is prevented in CCCP conditions. Data represent the mean ± SEM, n= 4, Student's t-test *P<0.05.

Figure 5: *Neurod1* overexpression rescues the mitochondrial deficit of adult-born hippocampal neurons of APPxPS1 mice. (a) Illustration of the somatic and distal dendritic compartments of adult-born granule neurons where mitochondrial content was assessed**.** (**b**) Confocal projections of the soma of GFP-labeled (GFP+) adult-born neurons of NTg and APPxPS1 mice injected with retroviral vectors expressing GFP alone (R-GFP) or both GFP and *Neurod1* (R-Neurod1) showing their mitochondrial content after immunochemistry of OXPHOS (red) and GFP (green) (Bar=5 µm). (**c**) Volume occupied by mitochondria per volume of GFP+ soma (mitochondrial biomass index, see methods) and (**d**) number of mitochondria in 14 and 21 dpi. Somatic mitochondrial biomass is altered early in new neurons of APPxPS1 mice. This alteration is abolished upon overexpression of *Neurod1*. Data represent the mean ± SEM, n=4-5 mice/group/time-point, one-way ANOVA (*P<0.05;

P<0.01). **(e) Confocal projections of dendritic segments of GFP+ new neurons (green) and their mitochondrial content revealed by OXPHOS immunostaining (red) (Bar=3 µm). **(f)** Dendritic mitochondrial biomass index and (**g**) number of dendritic mitochondria in 14 and 21 dpi GFP+ neurons of NTg and APPxPS1 mice injected with R-GFP or R-*Neurod1* vectors. Dendritic mitochondria biomass index is reduced in APPxPS1 compared to control mice at 21 dpi. Overexpression of R-*Neurod1* in APPxPS1 new neurons rescues this deficit through an increase in number of mitochondria. Data represent the mean ± SEM, n=3-4 mice/group/time-point, one-way ANOVA *P<0.05; **P<0.01; ***P<0.001.

Figure 6: *Neurod1* overexpression increases the number of spines associated with a mitochondria in adult-born hippocampal neurons. (a) Distribution across the different subtypes of dendritic spines coating adult-generated neurons in NTg and APPxPS1 mice. *Neurod1* overexpression overcomes the dendritic spine deficit of APPxPS1 mice. Data represent the mean ± SEM, n=4-5 mice/group/time-point; two-way ANOVA, *P<0.05; **P<0.01; ***P<0.001. **(b)** Three-dimensional reconstruction of a typical headed spine associated with a mitochondrion (Bar =2 µm). (**c**) Percentage of stubby, thin and mushroom spines associated with a mitochondrion at the basis of their neck, in NTg and APPxPS1 mice 21 days after R-GFP or R-*Neurod1* vectors injection. Overexpression of *Neurod1* increases the number of mitochondria-associated spines in adult-born hippocampal neurons. Data represent the mean ± SEM, n= 15–30 neurons/group, one-way ANOVA *P<0.05; **P<0.01.

Figure 1

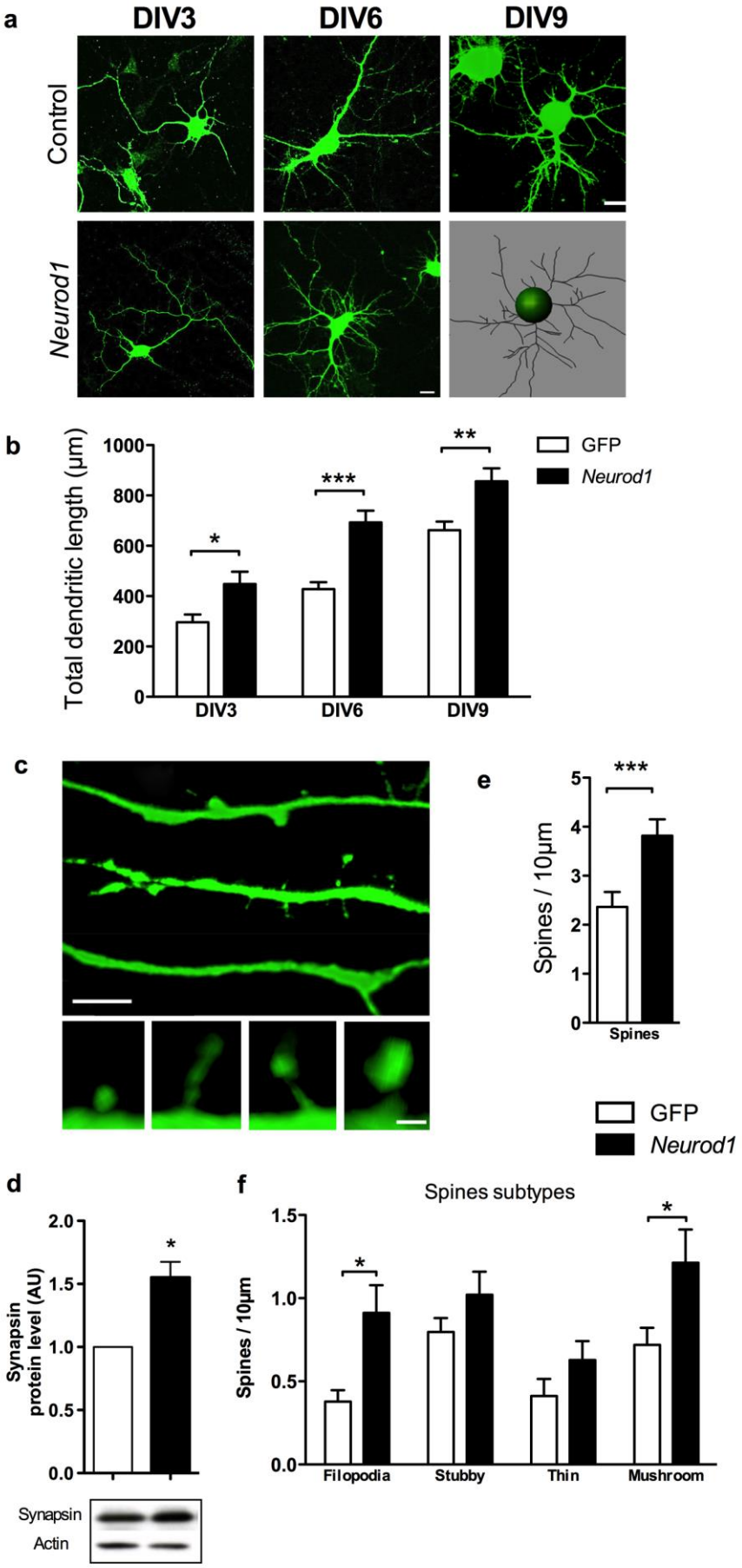

Figure 2

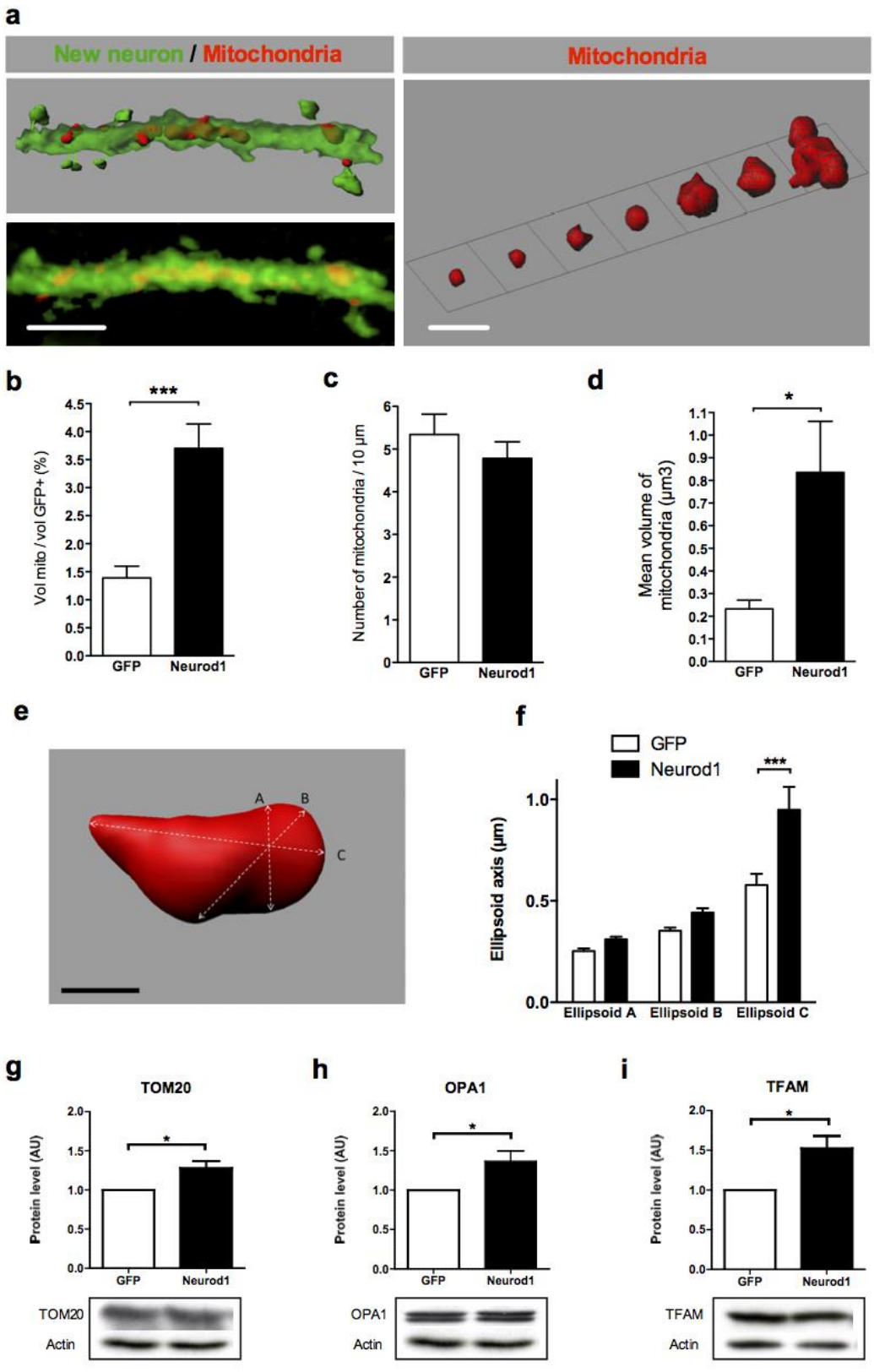

Figure 3

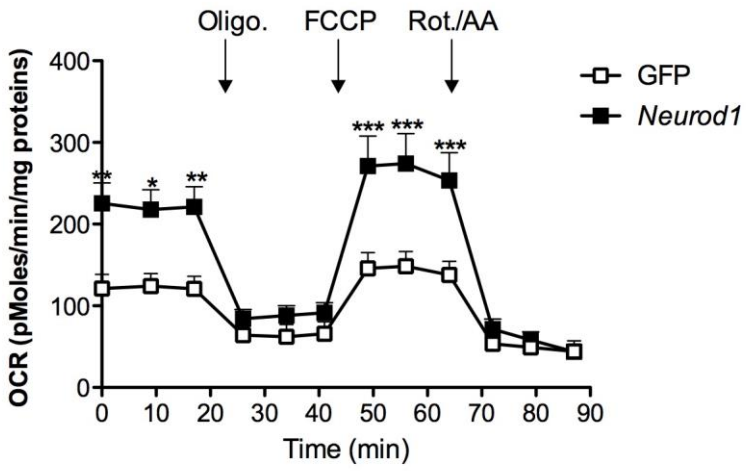

Figure 4

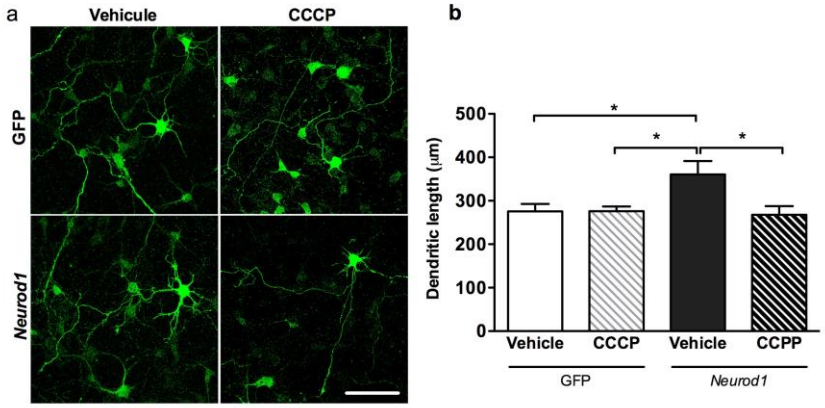

Figure 5

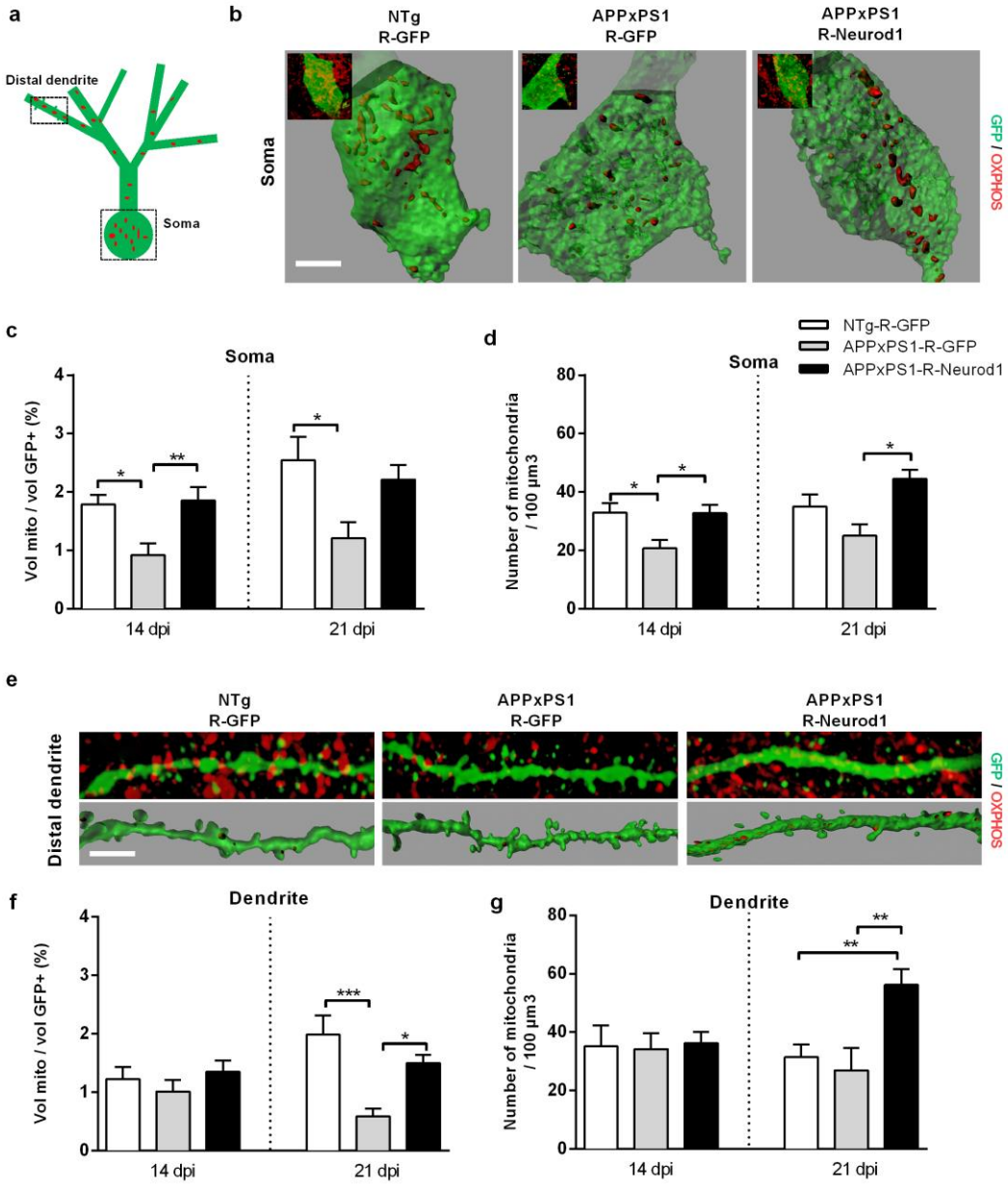

Figure 6

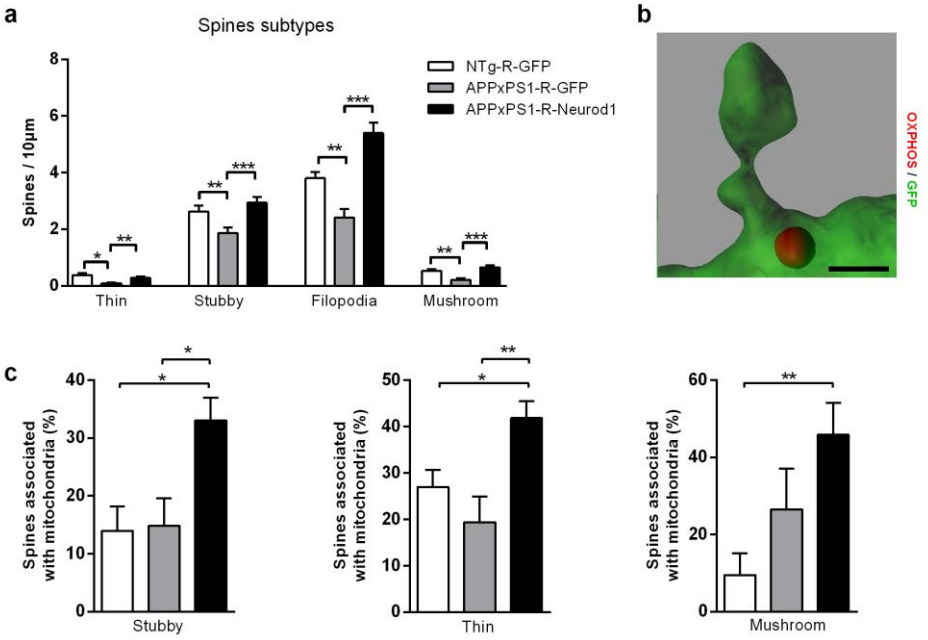

Amplifying mitochondrial function

rescues adult neurogenesis in a mouse model of Alzheimer's disease

Authors: Kevin Richetin[1], Manon Moulis[1], Aurélie Millet[1], Macarena S. Arràzola[1], Trinovita Andraini[1,2], Jennifer Hua[1], Noélie Davezac[1], Laurent Roybon[3], Pascale Belenguer[1], Marie-Christine Miquel[1#] and Claire Rampon[1#]*

Highlights:

- Altered dendritic spines density on APPxPS1 mice adult-born neurons
- Impaired mitochondrial content of APPxPS1 mice adult-born neurons
- Overexpression of Neurod1 rescues spine density and mitochondrial content
- Manipulating mitochondrial function may be used as therapeutic strategy